www.czasopisma.pan.pl PAN POLSKA AKADEMIA NAUK www.journals.pan.pl

Metrol. Meas. Syst., Vol. XXI (2014), No. 4, pp. 759–770.

PAN POLSKA AKADEMIA NAUK

METROLOGY AND MEASUREMENT SYSTEMS

Index 330930, ISSN 0860-8229

www.metrology.pg.gda.pl

M&MS

EXPERIMENTAL ANALYSIS BY MEASUREMENT OF SURFACE ROUGHNESS VARIATIONS IN TURNING PROCESS OF DUPLEX STAINLESS STEEL

Grzegorz M. Krolczyk[1)], Stanisław Legutko[2)]

1) Opole University of Technology, Faculty of Production Engineering and Logistics, Proszkowska 76, 45-758 Opole, Poland, (✉ g.krolczyk@po.opole.pl, +48 77 449 8688)

2) Poznan University of Technology, Faculty of Mechanical Engineering and Management, Piotrowo 3, 60-965 Poznan, Poland, (stanislaw.legutko@put.poznan.pl, +48 61 665 25 77)

Abstract

The objective of the investigation was to identify surface roughness after turning with wedges of coated sintered carbide. The investigation included predicting the average surface roughness in the dry machining of Duplex Stainless Steel (DSS) and the determination of load curves together with roughness profiles for various cutting conditions. The load curves and roughness profiles for various cutting wedges and variable cutting parameters were compared. It has been shown that dry cutting leads to a decrease in friction for lubricated surfaces, providing a small initial contact area where the surface is contacted. The study has been performed within a production facility during the production of electric motor parts and deep-well pumps.

Keywords: turning, coatings, friction-reducing, optical microscopy, surface roughness analysis and models.

1. Introduction

Engineering surfaces, particularly those generated using multi-step manufacturing processes and intended for tribological applications such as bearings and gears, rarely if ever have perfectly normal distributed elevations [1]. Surface roughness measurements of any workpiece are among the most important ones in length and angle metrology, both in theory and practice. According to Wieczorowski et al. [2], there are great discrepancies in these measurements because of the large variety of instruments for surface roughness analysis. Hence, three-dimensional surface topography parameters are necessary for assessing the surface roughness characteristics more effectively [3]. According to Mahovic Poljacek et al. [4], a precise characterization of roughness and surface topography is of prime importance in many engineering industries because certain functional properties of the materials are often determined by the surface structure and characteristics. Estimation of the magnitude of surface roughness under the given cutting conditions resulting from metal removal operations is one of the major goals in this area [5, 6]. According to Benardos and Vosniakos [7], surface roughness is a widely used index of product quality and in most cases a technical requirement for mechanical products. Achieving the desired surface quality is of great importance for the functional behaviour of a part.

Surface profilometry is for many years a well-known method of topography inspection [8–12]. Topography parameters represent surface properties is much better than 2D ones. Using the surface parameters can be determined functions describing surface behaviour. The workpiece material is duplex stainless steel because this stainless steel is widely used for many industrial applications due to its unique properties. Cabrera et al. [13] and Park et al. [14] consider that the good combination of their mechanical properties (high strength and toughness) and corrosion resistance makes them of great interest for a wide range of

Article history: received on Apr. 04, 2013; accepted on Sep. 21, 2014; available online on Dec. 15, 2014; DOI: 10.2478/mms-2014-0060.

applications, especially in the oil, chemical, and power industry. The aim of this study was to predict the surface roughness in dry and lubricated machining and compare the results of the surface roughness average for different cutting conditions, based on the rotatable central composite design of experiments. The machinability of duplex stainless steels has been dealt by many researchers [15−27], but those publications didn't mention about problems related to the 3D Functional Parameters of Surface Integrity (SI). 2D geometrical parameters of SI are important in determining corrosion resistance, and also in fatigue crack initiation. According to Rech and Moisan [28], examination of the machined surfaces using surface profilometry reveals the dependence of surface roughness on the tool radius as well as on the feed rate. This kind of surface is forbidden for a number of applications (oil tightness), but does not concern gear cone brakes, and can be avoided with additional abrasive processes such as lapping. This publication, describing various methods of the material ratio curve, is based on the material ratio curve. Pawlus and Grabon [29] consider that the Abbott curve is usually used to quantify wear phenomena such as lubricant influence, the bearing materials, and surface topography. They have shown that the wear measurement method for some types of engineering surfaces was developed based only on truncated surface measurements.

2. Experimental techniques

2.1. Workpiece and cutting tool materials

The machined material was 1.4462 (DIN EN 10088-1) steel with a ferritic-austenitic structure containing ca 50% of austenite. The elemental composition of the machined material and technical details of the cutting tools are given in Tables 1 and 2 respectively.

Table 1. Chemical composition of 1.4462 duplex stainless steel.

Element	%C max	%Si	%Mn	%P	%S	%Cr	%Ni	%Mo	%N	Others
wt%	0.021	0.54	0.77	0.028	0.02	22.65	5.70	3.28	0.19	-

Table 2. Cutting tool specification.

Tool	Substrate	Others
T1 MM 2025	Hardness: 1350 HV3 Grade: M25, P35	Coatings: Ti(C,N) - (2 μm); Al_2O_3 - (1.5 μm); TiN - (2 μm) Coating technique: CVD
T2 CTC 1135	Grade: M35, P35	Coatings: TiN - (2 μm); Ti(C,N) - (2 μm); Ti(N,B) - (2 μm); TiN - (2 μm); Ti(C,N) - (2 μm); Ti(C,N) - (2 μm) Coating technique: CVD

Cutting tool inserts of TNMG 160408 designation clamped in the tool shank of ISO-MTGNL 2020-16 type were employed. Based on the industry recommendations the range of cutting parameters T1: v_C = 50 ÷ 150 m/min, f = 0.2 ÷ 0.4 mm/rev, a_p = 1 ÷ 3 mm were selected. The experiments performed with the tool point T2 were comparative studies and that is why the cutting parameters were: v_C = 50, 100 and 150 m/min, f = 0.2, 0.3 and 0.4 mm/rev, a_p = 2 mm. The cutting wedges have been selected for various coating materials while the machining parameters selection was determined by the necessity to assess the finishing surface. The study was conducted within a production facility. The research program was carried out on a lathe CNC 400 CNC Famot - Pleszew.

2.2. The research plan of the surface roughness

The required number of experimental points is $N = 2^3 + 6 + 6 = 20$ (Table 3). There are eight factorial experiments (3 factors on two levels, 2^3) with added 6 star points and centre

Metrol. Meas. Syst., Vol. XXI (2014), No. 4, pp. 759–770.

point (average level) repeated 6 times to calculate the pure error [30]. For the purpose of the experiment a program that estimates parameters of the model second-order polynomial in the form $y = (a_0 + a_1*x_1 + a_2*x_2 + a_3*x_3)^2$ has been developed. The program was written in Matlab and it allows generating three-dimensional graphs and plots of one variable. The tests were performed on a CNC lathe, hence the test plan had been adjusted for the GE Fanuc Series 0 - T controlled machine program.

Table 3. Coded indication of the design of experiment.

Test No.	Coded values of factors			Real values of factors		
	x_1	x_2	x_3	v_C m/min	f mm/rev	a_p mm
1	-1	-1	-1	70	0.24	1.4
2	-1	-1	+1	70	0.24	2.6
3	-1	+1	-1	70	0.36	1.4
4	-1	+1	+1	70	0.36	2.6
5	+1	-1	-1	130	0.24	1.4
6	+1	-1	+1	130	0.24	2.6
7	+1	+1	-1	130	0.36	1.4
8	+1	+1	+1	130	0.36	2.6
9	-1.682	0	0	50	0.3	2
10	1.682	0	0	150	0.3	2
11	0	-1.682	0	100	0.2	2
12	0	1.682	0	100	0.4	2
13	0	0	-1.682	100	0.3	1
14	0	0	1.682	100	0.3	3
15	0	0	0	100	0.3	2
16	0	0	0	100	0.3	2
17	0	0	0	100	0.3	2
18	0	0	0	100	0.3	2
19	0	0	0	100	0.3	2
20	0	0	0	100	0.3	2

Based on the program presented in Table 3, and the experimental data set describing the mathematical model by means of a second-order polynomial function surface roughness *Ra* parameter after T1 turning, with respect to the turning process parameters, has been designated. The selection of the PS/DS-P: λ program was based on the assumption that the model of a second-order polynomial function will be a non-linear one which can be reduced to a linear model. *Ra* parameter was selected because during the assessment of production process, *Ra* is the commonly used parameter of surface roughness.

2.3. Tool wear and surface roughness analysis

Tool wear and surface textures analysis of DSS performed using Infinite Focus Measurement Machine (IFM). IFM an optical 3D measurement device which allows the acquisition of datasets at a high depth of focus. The IFM 4.2 software version was used for the measurements. The cooling and lubricating fluid used was a coolant compatible with water, with no chlorine content, based on Blasocut 4000CF mineral oils, a universal emulsion for medium hard machining of steel.

3. Results and discussion

3.1. Surface roughness

Figure 1 shows the surface roughness after machining DSS with T1 tool with Al_2O_3 layer under dry cutting conditions. The results were obtained by modelling on the basis of the adopted program: PS/DS - P: λ was presented as a three-dimensional plot and two plots of one variable in sequence showing the depth of cut and cutting speed for the parameters from the centre point. For cutting speed, v_C = 100 m/min and cutting depth, a_p = 2 mm, surface roughness, Ra, reaches the highest value in accordance with the theory of machining for the largest feed under investigation. In the feed range from 0.2 to 0.4 mm/rev the surface roughness changes its value from 1.2 to 6.6 µm. On the other hand, with a cutting speed of v_C = 100 m/min and a feed of f = 0.3 mm/rev of the surface roughness, *Ra* has the largest values for the cutting depth of a_p =1 mm and a_p = 3 mm and reaches 4.2 µm and 4.1 µm, respectively. The minimum value of the surface roughness *Ra* = 4 µm has been found for a cutting depth of a_p = 2.3 mm.

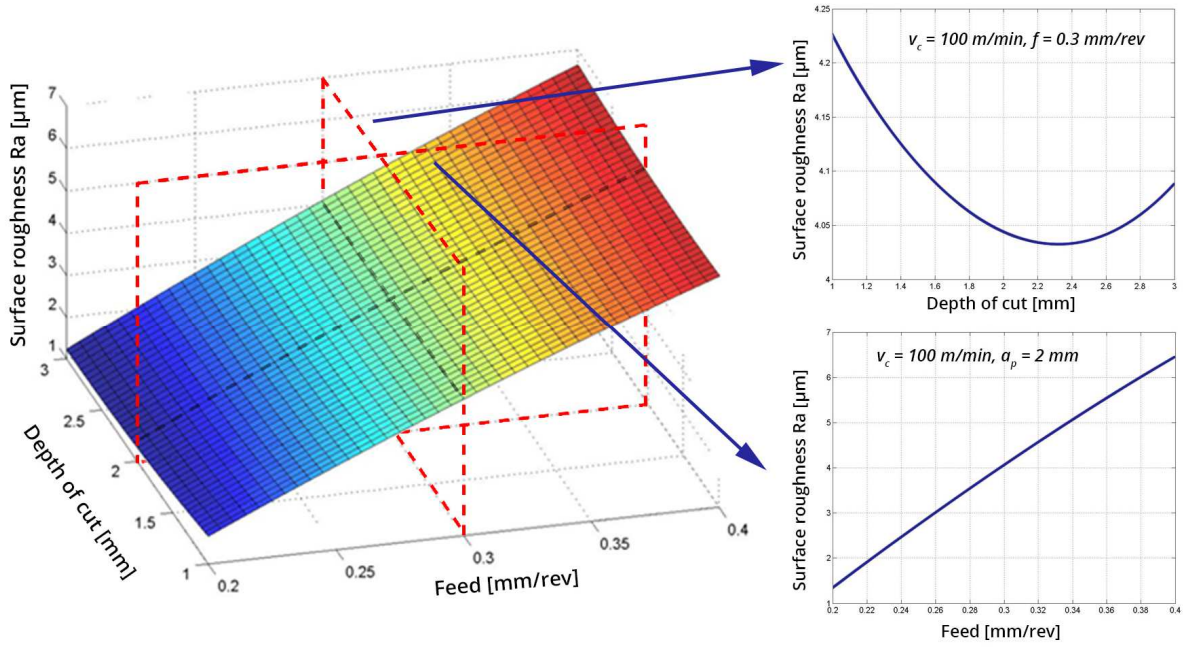

Fig. 1. Surface roughness for centre point parameters (T1) for constant cutting speed v_C = 100 m/min.

The effect of the feed rate and cutting speed on the surface roughness for T1 and T2 wedges are shown in Fig. 2 and 3. Generally it can be seen that by increasing the feed rate, the surface roughness decreases for each of the feeds for both tools. For the T1 wedge, shown in Fig. 2, the increase of surface roughness is constant with the increasing feed rate. There is a feed rate increase in the range of 0.2 mm/rev to 0.3 mm/rev for the T2 wedge results when there is a slight increase in roughness; in the range of 0.3 mm/rev to 0.4 mm/rev the roughness increases by two times. It has been found that the influence of the cutting speed on the values of surface roughness, *Ra*, was principally small (Fig. 3), both for a wedge possessing a coating with an intermediate ceramic layer and for one with a multilayer coating. For both wedges, the results of the surface roughness, measurements were characterized by small scatter as the factors of variation have the values of 1% to 6%, except the measurement for wedge T1 for the smallest cutting parameters (v_C = 50 m/min; f = 0.2 mm/rev - 13%).

Metrol. Meas. Syst., Vol. XXI (2014), No. 4, pp. 759–770.

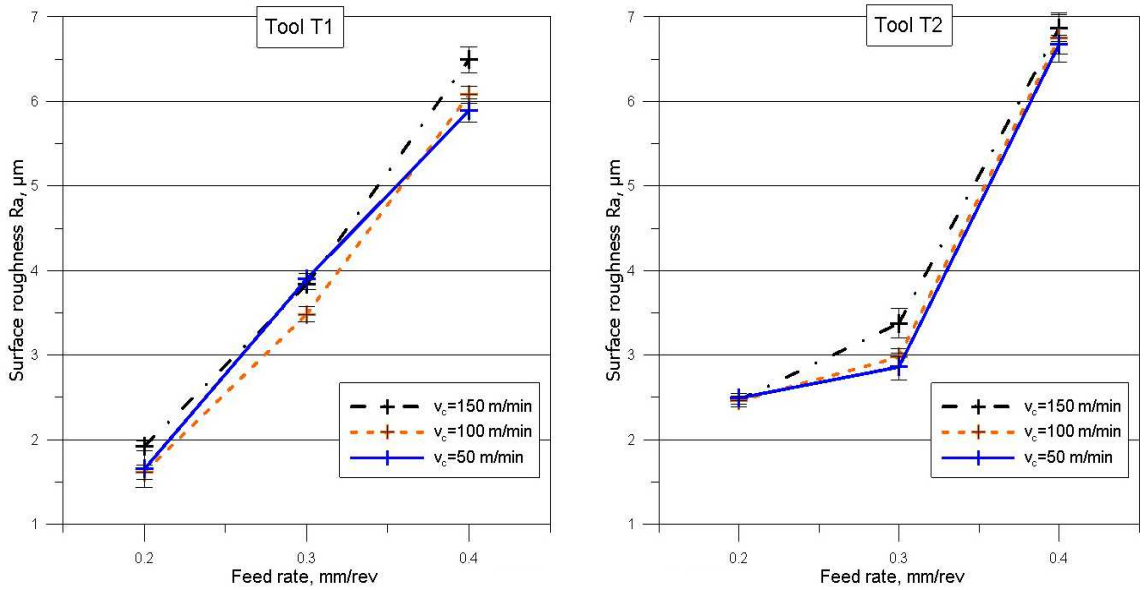

Fig. 2. Surface roughness *Ra* recorded in dry machining of DSS with both coated carbide tools as a function of feed rate; depth of cut $a_p = 2$ mm.

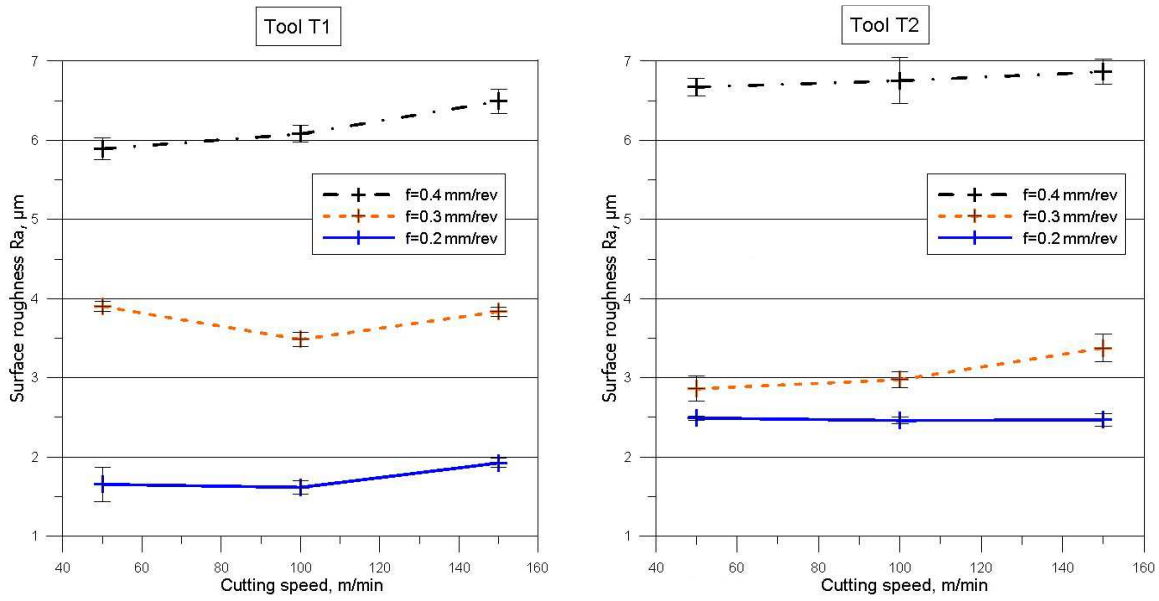

Fig. 3. Surface roughness *Ra* recorded in dry machining of DSS with both coated carbide tools as a function of cutting speed; depth of cut $a_p = 2$mm.

3.2. Surface texture

The surface texture analysis of DSS has been performed by means of an Infinite Focus Measurement Machine. The IFM is an optical 3D measurement device similar to the SEM. The IFM method allows for the capture of images with a lateral resolution down to 400 nm and a vertical resolution down to 20 nm. The geometrical structures of the surface shown below have been observed after longitude turning. This kind of machining has resulted in that the surface texture is a unidirectional perpendicular structure, which can be seen in Fig. 4. The figure shows the structure of a sample after turning with the parameters of the centre of the investigation program. The geometrical structure of the tested sample, together with the results of the measurements of the surface morphology parameters is shown in Figure 5.

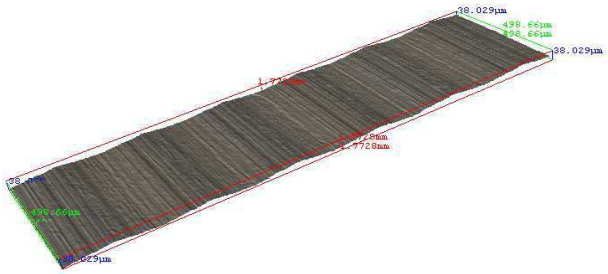

Fig. 4. Surface morphology of a sample turned with T1 wedge in real colour (v_C = 100 m/min; f = 0.3 mm/rev; a_p = 2 mm, dry).

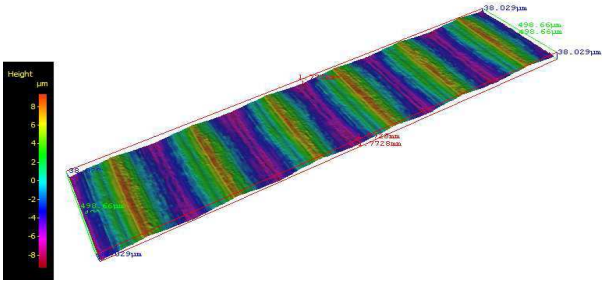

Fig. 5. Surface morphology of a sample turned with T1 wedge in pseudo colour (v_C = 100 m/min; f = 0.3 mm/rev; a_p = 2 mm, dry).

Machined surface has an anisotropic and periodical structure. A structure of this type occurs on contactless surfaces, mostly unloaded ones and co-acting with various kinds of wave interaction. This surface is often found in immobile contacts of indeformable bodies with deformable ones. A comparison of the load capacity curves (Abbott – Firestone Curve) depending on the cutting speed can be seen in Figure 6.

a)

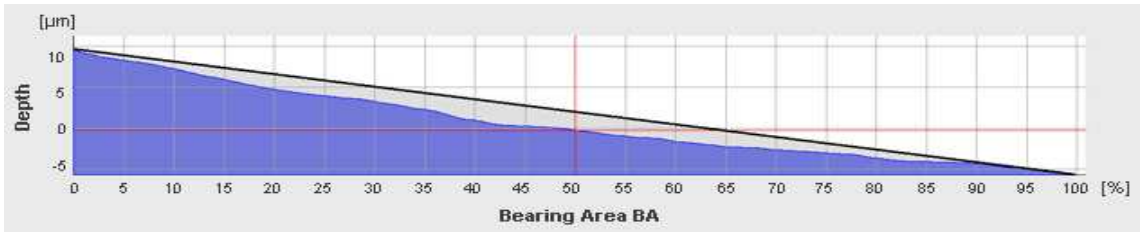

b)

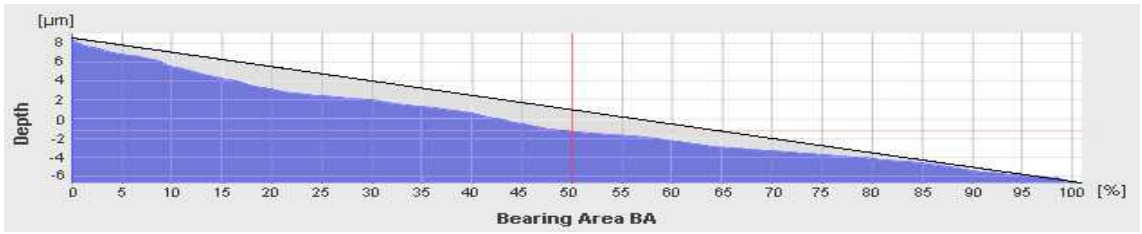

c)

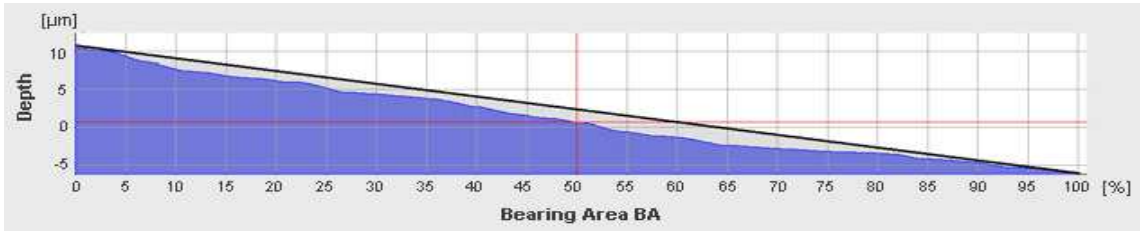

Fig. 6. Load capacity curves after turning with T1 wedge at the cutting speeds of: a) 50 m/min, b) 100 m/min, c) 150 m/min.

3.3. Profiles of surface roughness

Profiles of surface roughness after machining with various cutting speeds can be found in Figure 7. In this range, mainly large feed (f = 0.3 mm/rev) determines the characteristic, clearly periodical shape of the profile. The slopes of the analysed profiles differ in shape. The most irregular slopes are those of the profile for cutting speed of 150 m/min. A technological effect of so formed surface is, for example, a better oil adherence. This results in reduction of friction providing small initial contact surface. On the other hand, areas with significant values of contact stresses are obtained, which influences later utilization of machined parts manufactured in this way. Such technological parameters of machining result in arresting lubricating agents and contaminations on the surface.

Metrol. Meas. Syst., Vol. XXI (2014), No. 4, pp. 759–770.

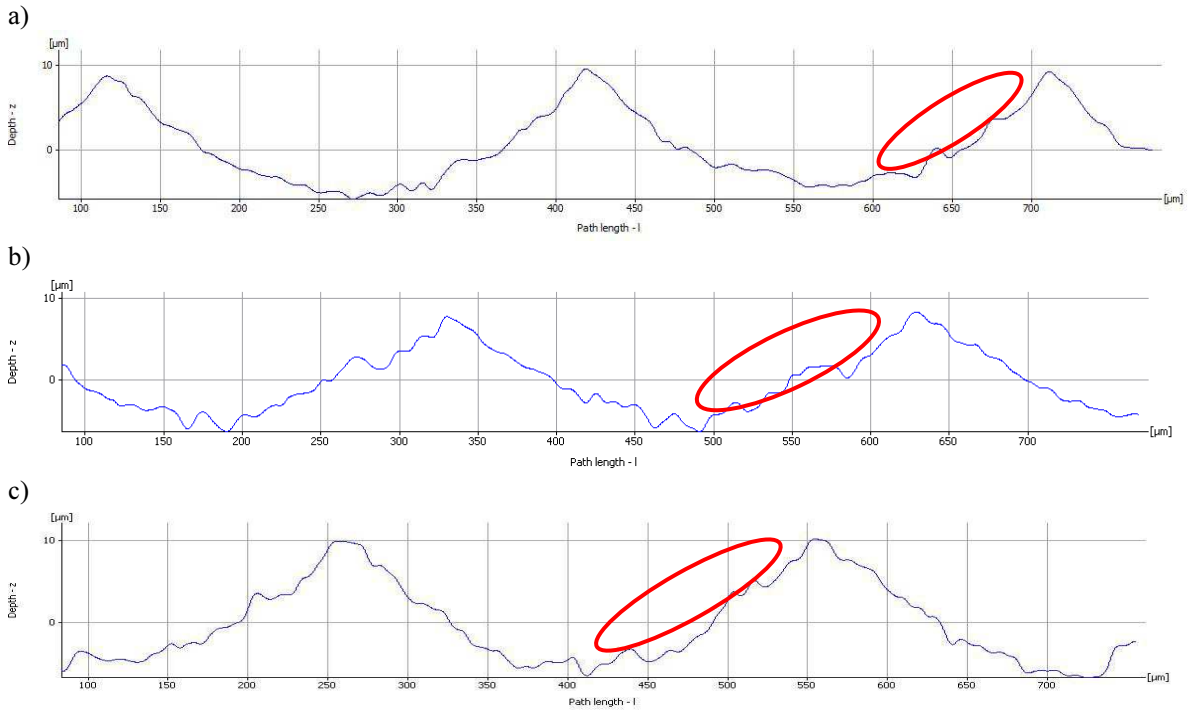

Fig. 7. Surface roughness profiles after turning with T1 wedge at the cutting speeds of: a) 50 m/min, b) 100 m/min, b) 150 m/min.

The shape of the load capacity curve mainly depends on the shape of irregularities in the direction perpendicular to the reference surface. It can be seen that the load capacity curves do not differ significantly from each other, hence the conclusion that the cutting speed does not significantly influence the load capacity curves in the process of turning duplex stainless steel. For all the cutting speed v_C obtained slightly degressive Abbott – Firestone Curves (grey colour area). Nielsen [31] found that the honing process can be controlled by *Rk* parameters. According to Sedlacek et al. [32], the *Rvk* and *Rpk* parameters could have an influence on friction. The representative measured values of roughness parameters and material ratio parameters (*Rk* parameters group) are listed in Tables 4 and 5.

Table 4. Roughness parameters for T1 tool.

Cutting speed [m/min]	*Ra* [µm]	*Rq* [µm]	*Rt* [µm]	*Rz* [µm]	*Rmax* [µm]	*Rp* [µm]	*Rv* [µm]	*Rc* [µm]
50, dry	3.58	4.28	15.20	8.68	11.80	9.51	5.69	15.20
100, dry	3.45	3.97	15.00	14.38	15.00	8.34	6.66	14.27
100, lubricated	4.34	4.90	16.80	12.78	15.43	9.07	7.72	16.53
150, dry	4.22	4.90	16.61	10.23	12.89	10.50	6.11	16.52

Table 5. Material ratio parameters for T1 tool.

Cutting speed [m/min]	*Rk* [µm]	*Rpk* [µm]	*Rvk* [nm]	*Rmr1* [%]	*Rmr2* [%]
50, dry	9.66	5.07	408.38	22.74	98.78
100, dry	9.85	4.49	516.97	17.48	98.53
100, lubricated	8.40	6.54	507.21	38.41	98.29
150, dry	11.37	4.40	270.57	24.03	98.29

Figures 8 and 9 are diagrams obtained from the measurements of duplex stainless steel samples turned with a T1 wedge and the use of a cooling substance. Figure 8 presents the load capacity curve of the sample turned with the centre parameters, with the use of a cooling fluid. Figure 9 shows the roughness profile of that sample.

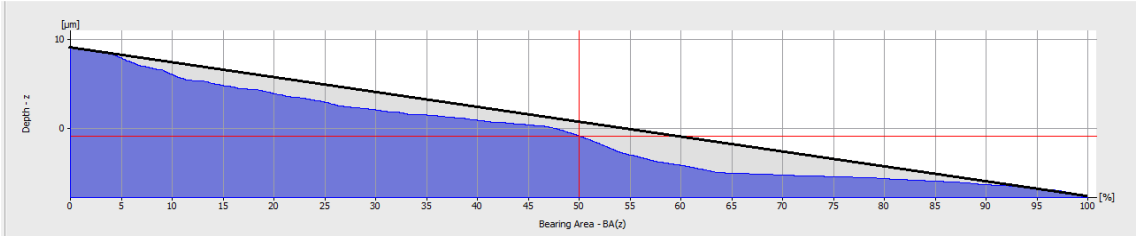

Fig. 8. Load capacity curve after turning with T1 wedge:
v_C = 100 m/min; f = 0.3 mm/rev; a_p = 2 mm, lubricated.

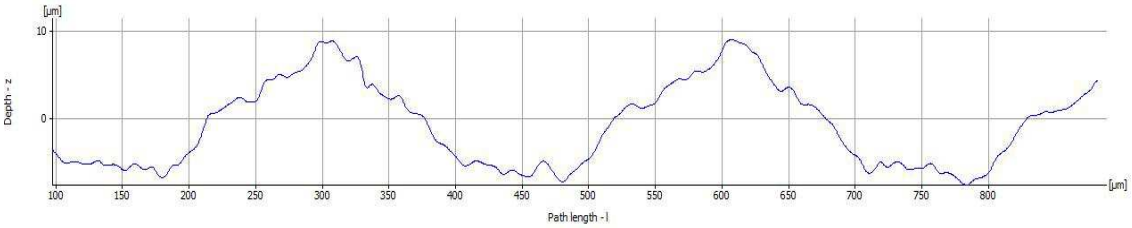

Fig. 9. Surface roughness profile after turning with T1 wedge:
v_C = 100 m/min; f = 0.3 mm/rev; a_p = 2 mm, lubricated.

As can be seen, the inclination angle of the middle part of the curve has decreased, but as much as to state that cooling advantageously influences the load capacity curve. The roughness profile of the surface has slightly deteriorated, which can be seen through small tribological disturbances. Roughness parameters and material ratio parameters for the T1 tool are listed in Tables 4 and 5.

Load capacity curves after the longitude turning of DSS with the T2 wedge, which have been shown in Figure 10. In the figure, one can observe the influence of cooling, which has an advantageous effect on the load capacity curve.

a)

b)

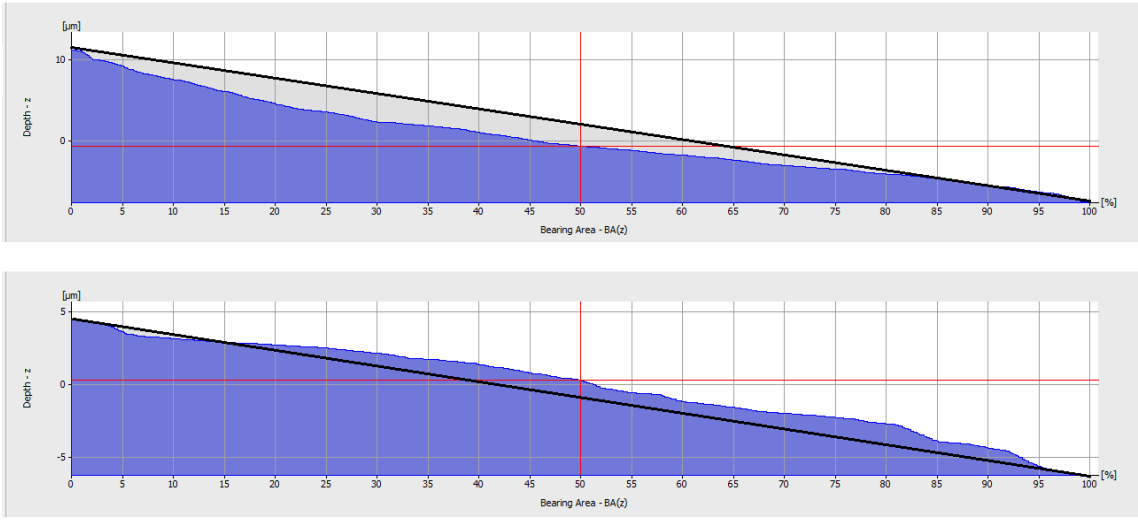

Fig. 10. Load capacity curves after turning with the T2 wedge:
v_C = 100 m/min; f = 0.3 mm/rev; a_p = 2 mm; a) without cooling, b) with the use of a cooling substance.

Analysing the roughness profiles shown in Figure 11, one can observe the visible influence of tribological disturbances. The disturbances probably have been caused by a built-up edge on the cutting edge and chip sticking on the rake face, and sticking of the machined material on the flank face. The roughness profile, after turning with the T2 wedge with cooling, on the other hand, shows many more tribological disturbances than in the case of machining without cooling. Lack of a lubricant caused greater tribological interferences also due to the built-up edge, but much less than in the case of cooling. It may be argued that there appears to be

Metrol. Meas. Syst., Vol. XXI (2014), No. 4, pp. 759–770.

a built-up edge and chipping on the flank wear probably with the occurrence of the hydrodynamic phenomena in the technological surface layer at the interface of the tool - the machined surface was the principal cause of the visible disturbance. The shape of the profile can also indicate a material side flow in the cutting zone. Kishawy and Elbestawi [33] thought that cutting with a small feed improves the surface finish. It leads to more material side flow on the machined surface and, hence, to a deterioration of the machined surface quality. In addition, increasing the tool nose radius leads to ploughing of a larger part of the chip and, hence, a severe material side flow takes place on the machined surface. Chip material flows in a direction perpendicular to that of the chip. This material sticks to the newly machined surface and causes damage to the machined surface quality, even if the surface roughness is kept within the desired tolerance [28]. Surface roughness parameters and material ratio parameters measured in this investigation are listed in Tables 6 and 7. Large *Rk* parameter in dry cutting for both tools implies a surface composed of high peaks providing small initial contact area and thus high areas of contact stress when the surface is contacted.

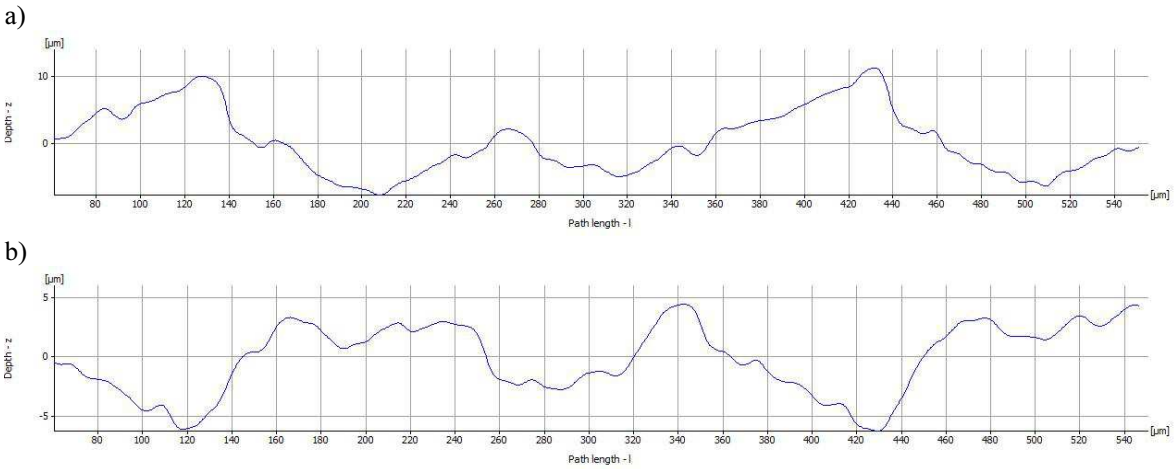

Fig. 11. Surface roughness profiles after turning with T2 wedge: v_C = 100 m/min; f = 0.3 mm/rev; a_p = 2 mm; a) without cooling, b) with the use of a cooling substance.

Table 6. Roughness parameters for T2 tool.

Cutting conditions	*Ra* [µm]	*Rq* [µm]	*Rt* [µm]	*Rz* [µm]	*Rmax* [µm]	*Rp* [µm]	*Rv* [µm]	*Rc* [µm]
dry	3.90	4.70	18.72	9.13	11.84	11.16	7.55	12.88
lubricated	2.52	2.91	10.71	6.17	7.86	4.44	6.26	8.39

Table 7. Material ratio parameters for T2 tool.

Cutting conditions	*Rk* [µm]	*Rpk* [µm]	*Rvk* [µm]	*Rmr1* [%]	*Rmr2* [%]
dry	11.40	5.71	1.08	18.41	95.85
lubricated	6.70	0.85	3.60	4.51	81.58

3.4. Tool wear

In order to explain shape of the roughness profiles shown in Figure 7 there was performed cutting tool points IFM images. Table 8 presents the condition of tool point surfaces using the corresponding IFM images. Figures a and c presents tool points in real colour, while figures b and d presents tool points in pseudo colour with tolerance changes to 10 µm. Red colour in Table 8 shows the areas where the cutting tool point in the machining process increase more than 10 µm of material, while the blue colour represents the surface of the cutting tool point which reduced more than 10 µm of material. It can be concluded that in the process of sliding friction between surfaces, some DSS particles were transferred to rake face near the tool point

– chip contact zone. These particles in the form of a built-up edge (BUE) are particularly visible on the rake face of the tool point with a cutting speed of 150 m/min. Reducing the cutting speed is 50 m/min resulted in the reduction of these phenomena. This type of wear is the result of mechanical action. Surface integrity of workpiece material easily harden, so each successive longitudinal turning pass at the same deep of cutting leads to the surface hardening, resulting in a more abrading. Furthermore flank wear on the rake face was observed. For cutting speed of 150 m/min flank wear is significantly higher than for the lower cutting speed. Flank wear and BUE on rake face probably caused irregular slopes on roughness profiles.

Table 8. Topography of the tool point wear in T1 during DSS turning.

a) 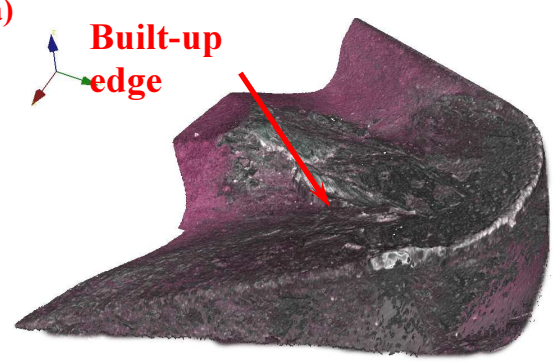 Topography of the tool point T1 in real colour (v_c = 50 m/min)	b) 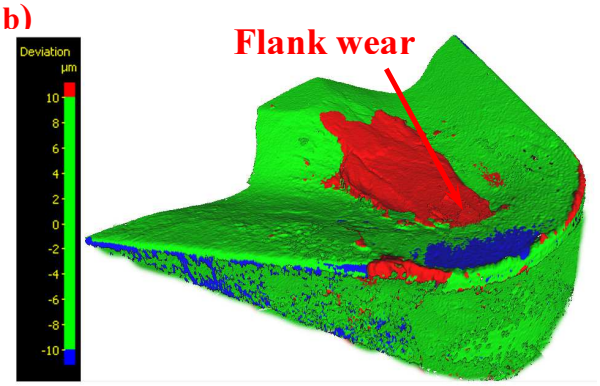 Topography of the tool point T1 in pseudo colour (v_c = 50 m/min)
c) 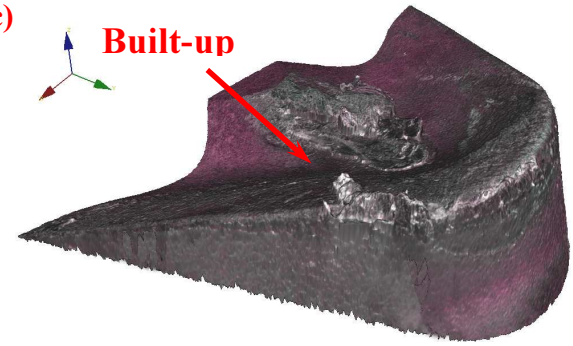 Topography of the tool point T1 in real colour (v_c = 150 m/min)	d) 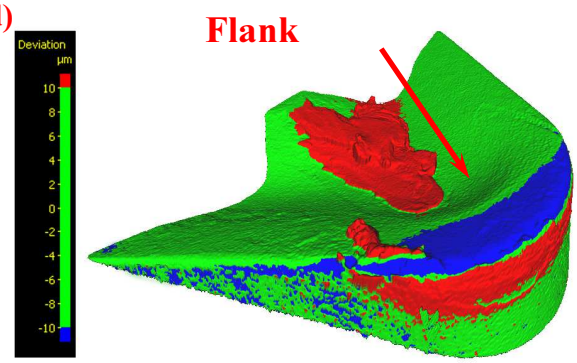 Topography of the tool point T1 in pseudo colour (v_c = 150 m/min)

3.5. Surface roughness model

Based on the PS/DS-P: λ program and the modelled experimental data of the polynomial function of surface roughness $Ra = f(v_C; f; a_p)$:

$$Ra = -1.716 - 0.013v_C + 27.518f + 1.431a_p - 0.00005v_C^2 - 15.979f^2 + 0.115a_p^2 + 0.047\, v_C f + 0.004\, v_C a_p + 1.458\, f a_p. \quad (1)$$

The aim was to create a model of such a tool to optimize cutting parameters for DSS which could be a valid for assumed turning parameters. A function model used to rationalize the selection of machining parameters (for real values) has not been verified in the range of cutting parameters beyond those adopted in Chapter 2.1. Since the function was verified in the production conditions, technologists employed in the industry, in order to determine the cutting parameters for the specified surface roughness in the process of turning DSS, may use

Metrol. Meas. Syst., Vol. XXI (2014), No. 4, pp. 759–770.

the designated model surface roughness. But we must remember about the limits of the tools and cutting methods.

4. Conclusions

During Duplex Stainless Steel machining, the following difficulties occur: difficulty in controlling the chip and strong adhesive interaction leading to the formation of a built-up edge. This leads to the following conclusions:

I. One can observe that the feed rate is the main parameter that influences the surface roughness, *Ra*. Surface roughness increased when increasing the feed rate. However, increasing the surface roughness, *Ra*, depends on the cutting tool specification.
II. In the process of turning Duplex Stainless Steel, the cutting speed does not significantly influence the load capacity curves.
III. The use of a mineral oil-based cooling and lubricating liquid advantageously influences the load capacity curve after turning with a multi-layer coated wedge.
IV. The roughness profile, after turning with a multi-layer coated wedge with cooling, show many more tribological disturbances than in the case of machining without cooling. The profile shape can prove a transverse plastic flow of the material in the cutting zone.
V. Dry cutting increases the *Rk* parameter – it leads to a decrease of friction providing a small initial contact area and thus high areas of contact stress when the surface is contacted. Dry cutting is associated with lubricant retention and debris entrapment.
VI. The developed surface roughness prediction model can be effectively used to predict the surface roughness for the turning process. Using such models, remarkable cost savings can be obtained.

References

[1] Cogdell, J. D. (2008). A convolved multi-Gaussian probability distribution for surface topography applications. *Precision Engineering*, 32, 34–46.

[2] Wieczorowski, M., Cellary, A., Majchrowski, R. (2010). The analysis of credibility and reproducibility of surface roughness measurement results. *Wear*, 269, 480–484.

[3] Ryu, S. H., Choi, D. K., Chu, C. N. (2006). Roughness and texture generation on end milled surfaces. *International Journal of Machine Tools & Manufacture*, 46, 404–412.

[4] Mahovic Poljacek, S., Risovic, D., Furic, K., Gojo, M. (2008). Comparison of fractal and profilometric methods for surface topography characterization. *Applied Surface Science*, 254, 3449–3458.

[5] Kukiełka, L. (2001). Mathematical modelling and numerical simulation of non-linear deformation of the asperity in the burnishing cold rolling operation. *Computational and Experimental Methods*, 5, 317–326.

[6] Kukiełka, L. (2002). Bases of engineering research. PWN, Warsaw.

[7] Benardos, P. G., Vosniakos, G. C. (2003). Predicting surface roughness in machining: a review, International Journal of Machine Tools & Manufacture, 43, 833–844.

[8] Wojciechowski, S., Twardowski, P., Wieczorowski, M. (2014). Surface texture analysis after ball end milling with various surface inclination of hardened steel. *Metrology and Measurement Systems*, 21(1), 145–56.

[9] Zawada-Tomkiewicz, A., Sciegienka R. (2011). Monitoring of a micro-smoothing process with the use of machined surface images, *Metrology and Measurement Systems*, 18(3), 419–428.

[10] Twardowski, P., Wojciechowski, S., Wieczorowski, M., Mathia, T.G. (2011). Selected Aspects of High Speed Milling Process Dynamics Affecting Machined Surface Roughness of Hardened Steel. *Scanning*, 33, 386–395.

[11] Krolczyk, G., Raos, P., Legutko, S. (2014). Experimental analysis of surface roughness and surface texture of machined and fused deposition modelled parts. *Tehnički Vjesnik - Technical Gazette*, 21, 217–221.

[12] Koszela, W., Pawlus, P., Rejwer, E., Ochwat, S. (2013). Possibilities of oil pockets creation by the burnishing technique. *Archives of Civil and Mechanical Engineering*, 13, 465–471.

[13] Cabrera, J. M., Mateo, A., Llanes, L., Prado, J. M., Anglada, M. (2003). Hot deformation of duplex stainless steels. *Journal of Materials Processing Technology*, 143–144, 321–325.

[14] Park, Y. H., Lee, Z. H. (2001). The effect of nitrogen and heat treatment on the microstructure and tensile properties of 25Cr–7Ni–1.5Mo–3W–xN duplex stainless steel castings. *Materials Science and Engineering: A*, 297, 78–84.

[15] Bouzid Saï, W., Lebrun, J. L. (2003). Influence of Finishing by Burnishing on Surface Characteristics. *Journal of Materials Engineering and Performance*, 12(1), 37–40.

[16] Braham-Bouchnak, T., Germain, G., Robert, P., Lebrun, J. L. (2010). High pressure water jet assisted machining of duplex steel: machinability and tool life. *International Journal of Material Forming*, 3, 507– 510.

[17] Ran, Q., Li, J., Xu, Y., Xiao, X., Yu, H., Jiang, L. (2013). Novel Cu-bearing economical 21Cr duplex stainless steels. Materials and Design, 46, 758–765.

[18] Nomani, J., Pramanik, A., Hilditch, T., Littlefair, G. (2013). Machinability study of first generation duplex (2205), second generation duplex (2507) and austenite stainless steel during drilling process. *Wear*, 304, 20–28.

[19] Krolczyk, G., Gajek, M., Legutko, S. (2013). Predicting the tool life in the dry machining of duplex stainless steel. *Eksploatacja i Niezawodnosc – Maintenance and Reliability*, 15(1), 62–65.

[20] Krolczyk, G., Legutko, S., Gajek, M. (2013). Predicting the surface roughness in the dry machining of duplex stainless steel (DSS). *Metalurgija*, 52(2), 259–262.

[21] Krolczyk, G., Gajek, M., Legutko, S. (2013). Effect of the cutting parameters impact on tool life in duplex stainless steel turning process. *Tehnički Vjesnik - Technical Gazette*, 20(4), 587–592.

[22] Krolczyk, G., Legutko, S., Raos, P. (2013). Cutting wedge wear examination during turning of duplex stainless steel, *Tehnički Vjesnik - Technical Gazette*, 20(3), 413–418.

[23] Krolczyk, G., Legutko, S., Stoic, A. (2013). Influence of cutting parameters and conditions onto surface hardness of duplex stainless steel after turning process. *Tehnički Vjesnik - Technical Gazette*, 20(6), 1077–1080.

[24] Krolczyk, G., Nieslony, P., Legutko, S., Stoic, A. (2014). Microhardness changes gradient of the Duplex Stainless Steel (DSS) surface layer after dry turning. *Metalurgija*, 53, 529–532.

[25] Selvaraj, D. P., Chandramohan, P., Mohanraj, M. (2014). Optimization of surface roughness, cutting force and tool wear of nitrogen alloyed duplex stainless steel in a dry turning process using Taguchi method. *Measurement*, 49, 205–215.

[26] Krolczyk, G., Nieslony, P., Legutko, S. (2014). Microhardness of Surface Integrity in turning process of duplex stainless steel (DSS) for different cutting conditions. Journal of Materials Engineering and Performance, 23(3), 859–866.

[27] Oliveira, C. A., Diniz, A. E., Bertazzoli, R. Correlating tool wear, surface roughness and corrosion resistance in the turning process of super duplex stainless steel. *Journal of the Brazilian Society of Mechanical Sciences and Engineering*, DOI 10.1007/s40430-013-0119-6.

[28] Rech, J., Moisan, A. (2003). Surface integrity in finish hard turning of case-hardened steels. *International Journal of Machine Tools & Manufacture*, 43(5), 543–550.

[29] Pawlus, P., Grabon, W. (2008). The method of truncation parameters measurement from material ratio curve. *Precision Engineering*, 32, 342–347.

[30] Montgomery, D. (2003). *Design and Analysis of Experiments*. 5th Edition, New York: John Wiley & Sons.

[31] Nielsen, H. S. (1988). New approaches to surface roughness evaluation of special surfaces. *Precision Engineering*, 10(4), 209–213.

[32] Sedlacek, M., Podgornik, B., Vizintin, J. (2009). Influence of surface preparation on roughness parameters, friction and wear. *Wear*, 266, 482–487.

[33] Kishawy, H. A., Elbestawi, M. A. (1999). Effects of process parameters on material side flow during hard turning. *International Journal of Machine Tools & Manufacture*, 39(7), 1017–1030.